Recent results on angular analysis of decay $B \to K^{*}\mu\mu$ at LHCb

Marcin Chrząszcz
mchrzasz@cern.ch

University of Zurich[UZH]

University of Padova
March 22, 2016

Outline

FIXME!

1. Why flavour is important.
2. $b \to s\ell\ell$ theory in a nutshell.
3. LHCb measurements of $b \to s\ell\ell$.
4. Global fit to $b \to s\ell\ell$ measurements.
5. Conclusions.

A lesson from history - GIM mechanism

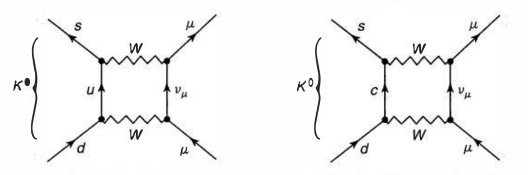

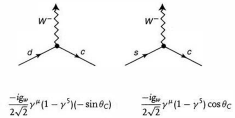

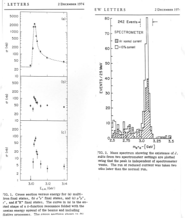

- Cabibbo angle was successful in explaining dozens of decay rates in the 1960s.
- There was, however, one that was not observed by experiments: $K^0 \to \mu^-\mu^+$.
- Glashow, Iliopoulos, Maiani (GIM) mechanism was proposed in the 1970 to fix this problem. The mechanism required the existence of the 4^{th} quark.
- At that point most of the people were skeptical about that. Fortunately in 1974 the discovery of the J/ψ meson silenced the skeptics.

A lesson from history - CKM matrix

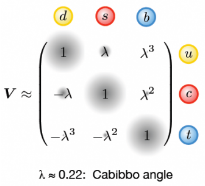

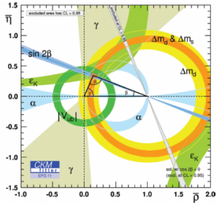

- Similarly CP violation was discovered in 1960s in the neutral kaons decays.
- 2×2 Cabbibo matrix could not allow for any CP violation.
- For the CP violation to be possible one needs at least a 3×3 unitary matrix ↬ Cabibbo-Kobayashi-Maskawa matrix (1973).
- It predicts existence of b (1977) and t (1995) quarks.

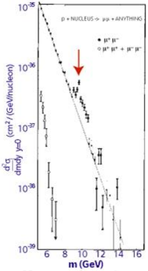

Results published in Physical Review Letters August 1, 1977

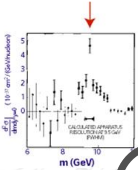

A lesson from history - Weak neutral current

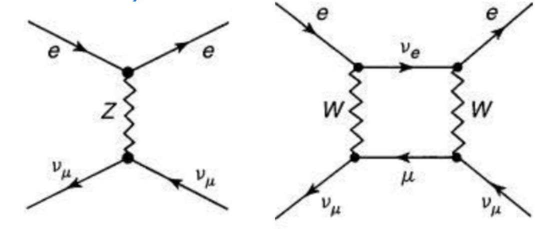

- Weak neutral currents were first, introduced in 1958 by Buldman.
- Later on they were naturally incorporated into unification of weak and electromagnetic interactions.
- ’t Hooft proved that the GWS models was renormalizable.
- Everything was there on theory side, only missing piece was the experiment, till 1973.

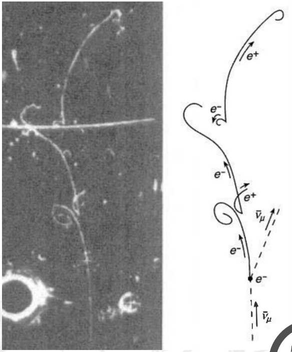

LHCb detector - tracking

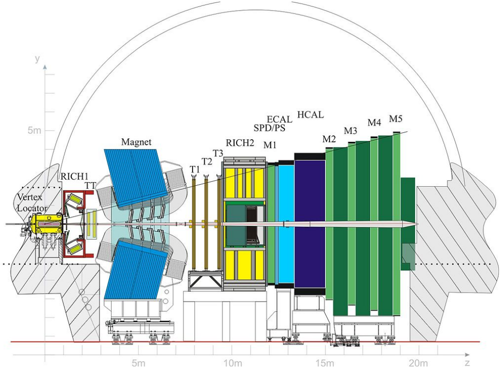

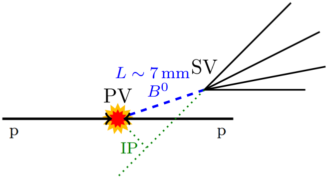

- Excellent Impact Parameter (IP) resolution ($20\ \mu$m).
  $\Rightarrow$ Identify secondary vertices from heavy flavour decays
- Proper time resolution $\sim\ 40$ fs.
  $\Rightarrow$ Good separation of primary and secondary vertices.
- Excellent momentum ($\delta p/p \sim 0.4 - 0.6\%$) and inv. mass resolution.
  $\Rightarrow$ Low combinatorial background.

LHCb detector - particle identification

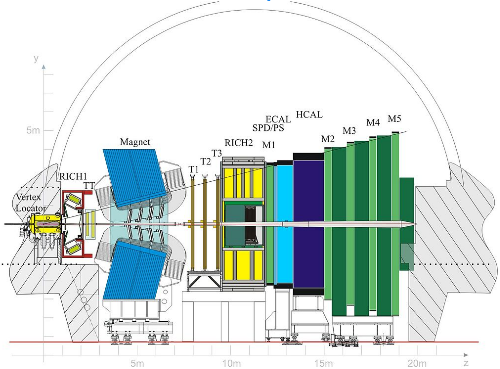

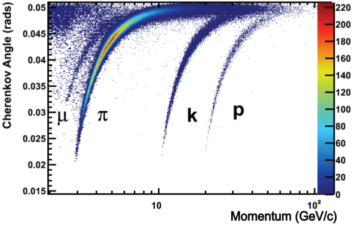

- Excellent Muon identification $\epsilon_{\mu\to\mu} \sim 97\%$, $\epsilon_{\pi\to\mu} \sim 1-3\%$
- Good $K-\pi$ separation via RICH detectors, $\epsilon_{K\to K} \sim 95\%$, $\epsilon_{\pi\to K} \sim 5\%$.
  $\Rightarrow$ Reject peaking backgrounds.
- High trigger efficiencies, low momentum thresholds. Muons: $p_T > 1.76\text{GeV}$ at L0, $p_T > 1.0\text{GeV}$ at HLT1,
  $B\to J/\psi X$: Trigger $\sim 90\%$.

Why rare decays?

- In SM allows only the charged interactions to change flavour.
  - Other interactions are flavour conserving.
- One can escape this constrain and produce $b \to s$ and $b \to d$ at loop level.
  - This kind of processes are suppressed in SM $\to$ Rare decays.
  - New Physics can enter in the loops.

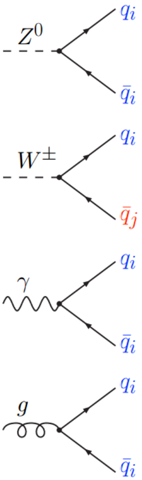

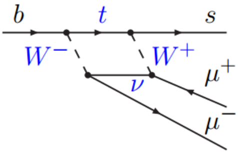

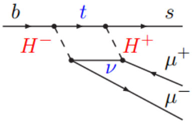

Tools in rare B^0 decays

- **Operator Product Expansion and Effective Field Theory**

$$H_{eff} = -\frac{4G_f}{\sqrt{2}} V V'^{*} \sum_i \Big[\underbrace{C_i(\mu) O_i(\mu)}_{\text{left-handed}} + \underbrace{C_i'(\mu) O_i'(\mu)}_{\text{right-handed}} \Big],$$

i=1,2	Tree
i=3-6,8	Gluon penguin
i=7	Photon penguin
i=9.10	EW penguin
i=S	Scalar penguin
i=P	Pseudoscalar penguin

where C_i are the Wilson coefficients and O_i are the corresponding effective operators.

$b \to s\gamma$

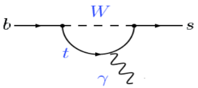

$C_7^{(\prime)}$

$b \to s\ell^+\ell^-$

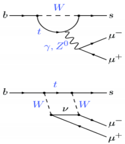

$C_7^{(\prime)}, C_9^{(\prime)}, C_{10}^{(\prime)}$

$B^0_{(s)} \to \mu^+\mu^-$

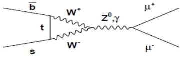

$C_S^{(\prime)}, C_P^{(\prime)}, C_{10}^{(\prime)}$

$B \to K^* \mu\mu$ as a golden channel

$B^0 \to K^*\mu^-\mu^+$ kinematics

⇛ The kinematics of $B^0 \to K^*\mu^-\mu^+$ decay is described by three angles θ_l, θ_k, ϕ and invariant mass of the dimuon system (q^2).

⇛ $\cos\theta_k$: the angle between the direction of the kaon in the K^* ($\overline{K^*}$) rest frame and the direction of the K^* ($\overline{K^*}$) in the B^0 ($\overline{B}^0$) rest frame.

⇛ $\cos\theta_l$: the angle between the direction of the μ^- (μ^+) in the dimuon rest frame and the direction of the dimuon in the B^0 ($\overline{B}^0$) rest frame.

⇛ ϕ: the angle between the plane containing the μ^- and μ^+ and the plane containing the kaon and pion from the K^*.

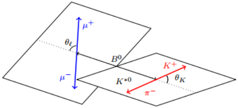

(a) θ_K and θ_ℓ definitions for the B^0 decay

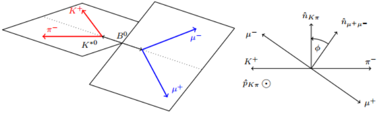

(b) ϕ definition for the B^0 decay

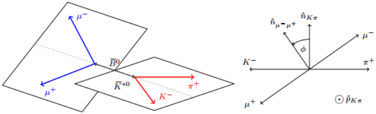

(c) ϕ definition for the $\overline{B}^0$ decay

$B^0 \to K^* \mu^- \mu^+$ kinematics

⇛ The kinematics of $B^0 \to K^* \mu^- \mu^+$ decay is described by three angles θ_l, θ_k, ϕ and invariant mass of the dimuon system (q^2).

$$\frac{d^4\Gamma}{dq^2\, d\cos\theta_K\, d\cos\theta_l\, d\phi} = \frac{9}{32\pi}\Big[J_{1s}\sin^2\theta_K + J_{1c}\cos^2\theta_K + (J_{2s}\sin^2\theta_K + J_{2c}\cos^2\theta_K)\cos 2\theta_l$$

$$+J_3\sin^2\theta_K\sin^2\theta_l\cos 2\phi + J_4\sin 2\theta_K\sin 2\theta_l\cos\phi + J_5\sin 2\theta_K\sin\theta_l\cos\phi$$

$$+(J_{6s}\sin^2\theta_K + J_{6c}\cos^2\theta_K)\cos\theta_l + J_7\sin 2\theta_K\sin\theta_l\sin\phi + J_8\sin 2\theta_K\sin 2\theta_l\sin\phi$$

$$+J_9\sin^2\theta_K\sin^2\theta_l\sin 2\phi\Big], \qquad (1)$$

⇛ This is the most general expression of this kind of decay.

Transversity amplitudes

$\Rrightarrow$ One can link the angular observables to transversity amplitudes

$$
\begin{aligned}
J_{1s} &= \frac{(2+\beta_\ell^2)}{4}\left[|A_\perp^L|^2+|A_\parallel^L|^2+|A_\perp^R|^2+|A_\parallel^R|^2\right]+\frac{4m_\ell^2}{q^2}\mathrm{Re}\left(A_\perp^L A_\perp^{R\,*}+A_\parallel^L A_\parallel^{R\,*}\right),\\
J_{1c} &= |A_0^L|^2+|A_0^R|^2+\frac{4m_\ell^2}{q^2}\left[|A_t|^2+2\mathrm{Re}(A_0^L A_0^{R\,*})\right]+\beta_\ell^2\,|A_S|^2,\\
J_{2s} &= \frac{\beta_\ell^2}{4}\left[|A_\perp^L|^2+|A_\parallel^L|^2+|A_\perp^R|^2+|A_\parallel^R|^2\right], \qquad J_{2c}=-\beta_\ell^2\left[|A_0^L|^2+|A_0^R|^2\right],\\
J_3 &= \frac{1}{2}\beta_\ell^2\left[|A_\perp^L|^2-|A_\parallel^L|^2+|A_\perp^R|^2-|A_\parallel^R|^2\right], \qquad J_4=\frac{1}{\sqrt{2}}\beta_\ell^2\left[\mathrm{Re}(A_0^L A_\parallel^{L\,*}+A_0^R A_\parallel^{R\,*})\right],\\
J_5 &= \sqrt{2}\beta_\ell\left[\mathrm{Re}(A_0^L A_\perp^{L\,*}-A_0^R A_\perp^{R\,*})-\frac{m_\ell}{\sqrt{q^2}}\mathrm{Re}(A_\parallel^L A_S^*+A_\parallel^{R\,*}A_S)\right],\\
J_{6s} &= 2\beta_\ell\left[\mathrm{Re}(A_\parallel^L A_\perp^{L\,*}-A_\parallel^R A_\perp^{R\,*})\right], \qquad J_{6c}=4\beta_\ell\frac{m_\ell}{\sqrt{q^2}}\mathrm{Re}(A_0^L A_S^*+A_0^{R\,*}A_S),\\
J_7 &= \sqrt{2}\beta_\ell\left[\mathrm{Im}(\mathrm{A_0^L A_\parallel^{L\,*}}-\mathrm{A_0^R A_\parallel^{R\,*}})+\frac{\mathrm{m}_\ell}{\sqrt{\mathrm{q}^2}}\mathrm{Im}(\mathrm{A_\perp^L A_S^*}-\mathrm{A_\perp^{R\,*}A_S}))\right],\\
J_8 &= \frac{1}{\sqrt{2}}\beta_\ell^2\left[\mathrm{Im}(\mathrm{A_0^L A_\perp^{L\,*}}+\mathrm{A_0^R A_\perp^{R\,*}})\right], \qquad J_9=\beta_\ell^2\left[\mathrm{Im}(\mathrm{A_\parallel^{L\,*}A_\perp^L}+\mathrm{A_\parallel^{R\,*}A_\perp^R})\right],
\end{aligned}
\tag{2}
$$

Link to effective operators

⇛ So here is where the magic happens. At leading order the amplitudes can be written as:

$$A_\perp^{L,R} = \sqrt{2} N m_B (1-\hat{s}) \left[(\mathcal{C}_9^{\rm eff} + \mathcal{C}_9^{\rm eff\prime}) \mp (\mathcal{C}_{10} + \mathcal{C}_{10}^\prime) + \frac{2\hat{m}_b}{\hat{s}} (\mathcal{C}_7^{\rm eff} + \mathcal{C}_7^{\rm eff\prime}) \right] \xi_\perp(E_{K^*})$$

$$A_\parallel^{L,R} = -\sqrt{2} N m_B (1-\hat{s}) \left[(\mathcal{C}_9^{\rm eff} - \mathcal{C}_9^{\rm eff\prime}) \mp (\mathcal{C}_{10} - \mathcal{C}_{10}^\prime) + \frac{2\hat{m}_b}{\hat{s}} (\mathcal{C}_7^{\rm eff} - \mathcal{C}_7^{\rm eff\prime}) \right] \xi_\perp(E_{K^*})$$

$$A_0^{L,R} = -\frac{N m_B (1-\hat{s})^2}{2\hat{m}_{K^*}\sqrt{\hat{s}}} \left[(\mathcal{C}_9^{\rm eff} - \mathcal{C}_9^{\rm eff\prime}) \mp (\mathcal{C}_{10} - \mathcal{C}_{10}^\prime) + 2\hat{m}_b (\mathcal{C}_7^{\rm eff} - \mathcal{C}_7^{\rm eff\prime}) \right] \xi_\parallel(E_{K^*}), \quad (3)$$

where $\hat{s} = q^2/m_B^2$, $\hat{m}_i = m_i/m_B$. The $\xi_{\parallel,\perp}$ are the form factors.

Link to effective operators

$\Rrightarrow$ So here is where the magic happens. At leading order the amplitudes can be written as:

$$A_{\perp}^{L,R} = \sqrt{2}Nm_B(1-\hat{s})\left[(\mathcal{C}_9^{\text{eff}}+\mathcal{C}_9^{\text{eff}\prime})\mp(\mathcal{C}_{10}+\mathcal{C}_{10}^{\prime})+\frac{2\hat{m}_b}{\hat{s}}(\mathcal{C}_7^{\text{eff}}+\mathcal{C}_7^{\text{eff}\prime})\right]\xi_{\perp}(E_{K^*})$$

$$A_{\parallel}^{L,R} = -\sqrt{2}Nm_B(1-\hat{s})\left[(\mathcal{C}_9^{\text{eff}}-\mathcal{C}_9^{\text{eff}\prime})\mp(\mathcal{C}_{10}-\mathcal{C}_{10}^{\prime})+\frac{2\hat{m}_b}{\hat{s}}(\mathcal{C}_7^{\text{eff}}-\mathcal{C}_7^{\text{eff}\prime})\right]\xi_{\perp}(E_{K^*})$$

$$A_{0}^{L,R} = -\frac{Nm_B(1-\hat{s})^2}{2\hat{m}_{K^*}\sqrt{\hat{s}}}\left[(\mathcal{C}_9^{\text{eff}}-\mathcal{C}_9^{\text{eff}\prime})\mp(\mathcal{C}_{10}-\mathcal{C}_{10}^{\prime})+2\hat{m}_b(\mathcal{C}_7^{\text{eff}}-\mathcal{C}_7^{\text{eff}\prime})\right]\xi_{\parallel}(E_{K^*}), \quad (3)$$

where $\hat{s}=q^2/m_B^2$, $\hat{m}_i=m_i/m_B$. The $\xi_{\parallel,\perp}$ are the form factors.

$\Rrightarrow$ Now we can construct observables that cancel the ξ form factors at leading order:

$$P_5^{\prime}=\frac{J_5+\bar{J}_5}{2\sqrt{-(J_2^c+\bar{J}_2^c)(J_2^s+\bar{J}_2^s)}} \quad (4)$$

LHCbs $B^0 \to K^*\mu^-\mu^+$, Selection

⇛ Trigger

- Muon trigger.
- Topological trigger.

⇛ Good modelling with MC.

⇛ Selection:

- As loose as possible.
- Based on the B^0 vertex quality, impact parameters, loose Particle identification for the hadrons.
- The variables were chosen in a way we are sure the are correctly modelled in MC.

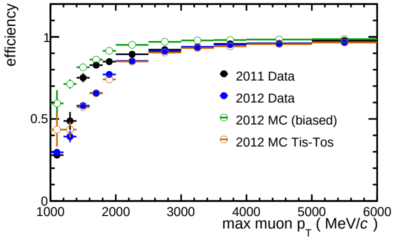

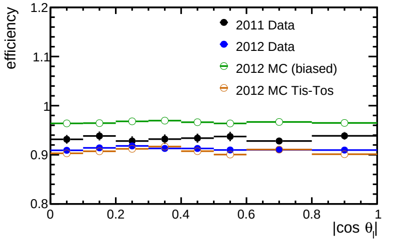

Peaking backgrounds

- ⇛ A number of peaking backgrounds that can mistaken as your signal.
- ⇛ There where a specially designed vetoes to fight each of them.

	after preselection, before vetoes		after vetoes and selection	
Channel	Estimated events	% signal	Estimated events	% signal
$\Lambda_b \to \Lambda^*(1520)^0\mu\mu$	$(1.0 \pm 0.5) \times 10^3$	19 ± 8	51 ± 25	1.0 ± 0.4
$\Lambda_b \to pK\mu\mu$	$(1.0 \pm 0.5) \times 10^2$	1.9 ± 0.8	5.7 ± 2.8	0.11 ± 0.05
$B_d^0 \to K^+\mu\mu$	28 ± 7	0.55 ± 0.06	1.6 ± 0.5	0.031 ± 0.006
$B_s^0 \to \phi\mu\mu$	$(3.2 \pm 1.3) \times 10^2$	6.2 ± 2.1	17 ± 7	0.33 ± 0.12
signal swaps	$(3.6 \pm 0.9) \times 10^2$	6.9 ± 0.6	33 ± 9	0.64 ± 0.06
$B_d^0 \to K^*J/\psi$ swaps	$(1.3 \pm 0.4) \times 10^2$	2.6 ± 0.4	2.7 ± 2.8	0.05 ± 0.05

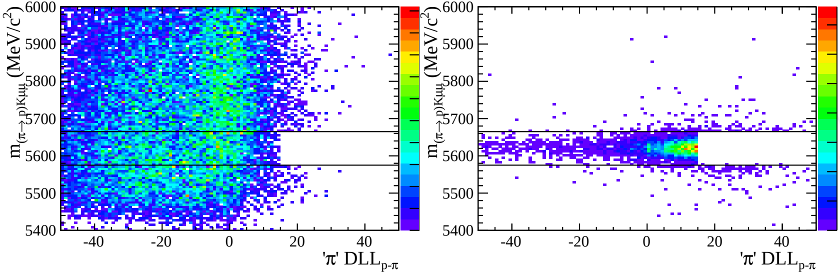

Multivariate simulation

- PID, kinematics and isolation variables used in a Boosted Decision Tree (BDT) to discriminate signal and background.
- BDT with k-Folding technique.
- Completely data drive.

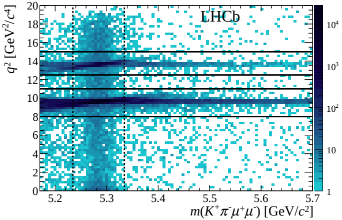

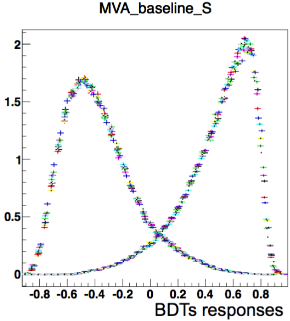

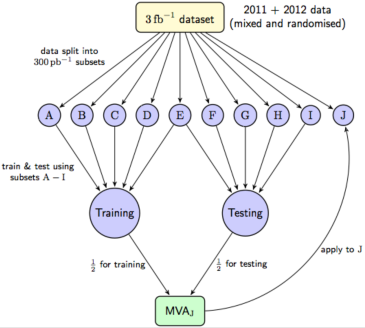

Multivariate simulation, efficiency

⇛ BDT was also check in order not to bias our angular distribution:

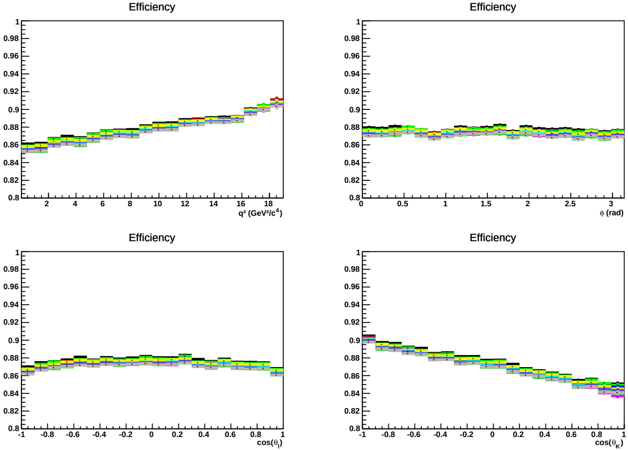

⇛ The BDT has small impact on our angular observables. We will correct for this effects later on.

Mass modelling

⇛ The signal is modelled by a sum of two Crystal-Ball function with common mean.
⇛ The background is a single exponent
⇛ The base parameters is performed in the proxy channel: $B_d^0 \to J/\psi(\mu\mu)K^*$.
⇛ All the parameters are fixed in the signal pdf.
⇛ Scaling factors for resolution are determined from MC.
⇛ In fitting the rare mode only the signal, background yield and the slope of the exponential is left floating.

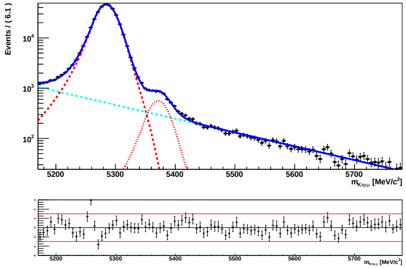

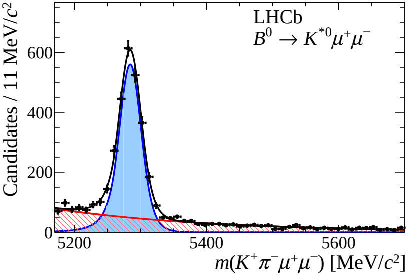

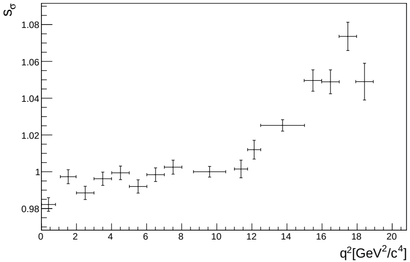

⇛ We got 624 ± 30 candidates in the most interesting $[1.1, 6.0]$ $\mathrm{GeV}^2/\mathrm{c}^4$ region and 2398 ± 57 in the full range $[1.1, 19.]$ $\mathrm{GeV}^2/\mathrm{c}^4$.

⇛ The S-wave fraction is extracted using a LASS model.

Monte Carlo corrections

⇛ No Monte Carlo simulation is perfect! One needs to correct for remaining differences.

⇛ We reweighed our $B_d^0 \to K^* \mu\mu$ Monte Carlo accordingly to differences between the $B_d^0 \to K^* J/\psi$ in data (Splot) and Monte Carlo.

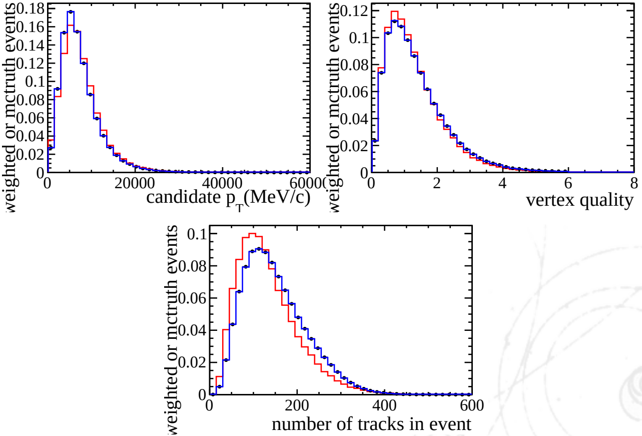

Monte Carlo corrections

⇛ No Monte Carlo simulation is perfect! One needs to correct for remaining differences.
⇛ We reweighed our $B_d^0 \to K^* \mu\mu$ Monte Carlo accordingly to differences between the $B_d^0 \to K^* J/\psi$ in data (Splot) and Monte Carlo.

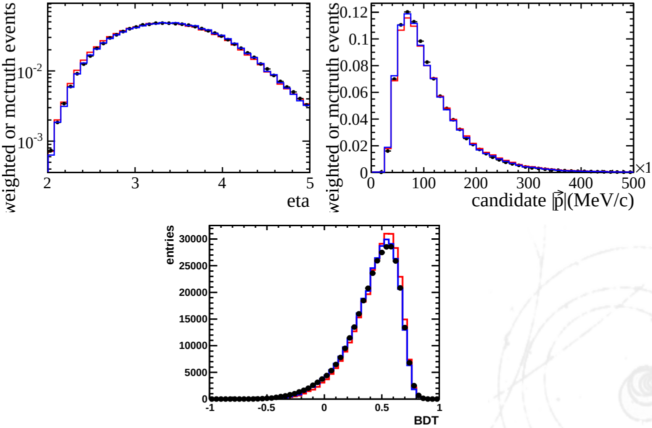

Detector acceptance

- Detector distorts our angular distribution.
- We need to model this effect.
- 4D function is used:

$$\epsilon(\cos\theta_l, \cos\theta_k, \phi, q^2) = \sum_{ijkl} P_i(\cos\theta_l) P_j(\cos\theta_k) P_k(\phi) P_l(q^2),$$

  where P_i is the Legendre polynomial of order i.
- We use up to $4^{th}, 5^{th}, 6^{th}, 5^{th}$ order for the $\cos\theta_l, \cos\theta_k, \phi, q^2$.
- The coefficients were determined using Method of Moments, with a huge simulation sample.
- The simulation was done assuming a flat phase space and reweighing the q^2 distribution to make is flat.
- To make this work the q^2 distribution needs to be reweighed to be flat.

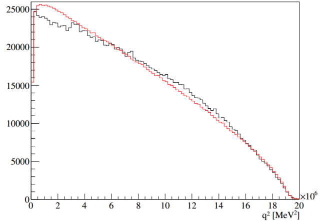

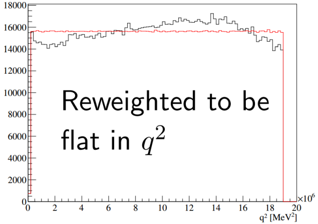

Detector acceptance

- Detector distorts our angular distribution.
- We need to model this effect.
- 4D function is used:

$$\epsilon(\cos\theta_l, \cos\theta_k, \phi, q^2) = \sum_{ijkl} P_i(\cos\theta_l) P_j(\cos\theta_k) P_k(\phi) P_l(q^2),$$

  where P_i is the Legendre polynomial of order i.
- We use up to $4^{th}, 5^{th}, 6^{th}, 5^{th}$ order for the $\cos\theta_l, \cos\theta_k, \phi, q^2$.
- The coefficients were determined using Method of Moments, with a huge simulation sample.
- The simulation was done assuming a flat phase space and reweighing the q^2 distribution to make is flat.
- To make this work the q^2 distribution needs to be reweighed to be flat.

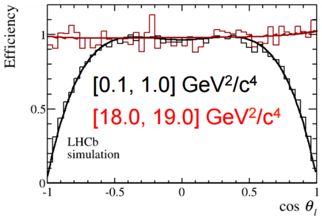

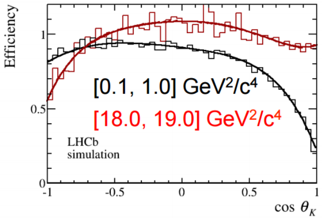

Control channel

- We tested our unfolding procedure on $B \to J/\psi K^*$.
- The result is in perfect agreement with other experiments and our different analysis of this decay.

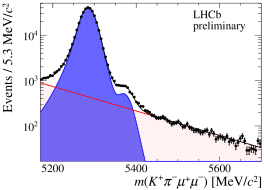

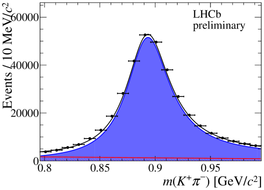

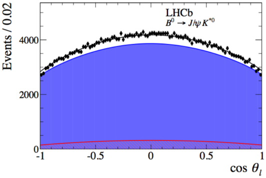

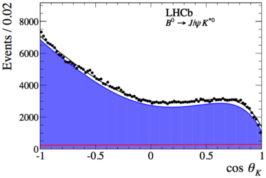

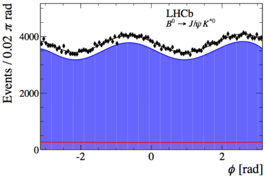

The columns of New Physics

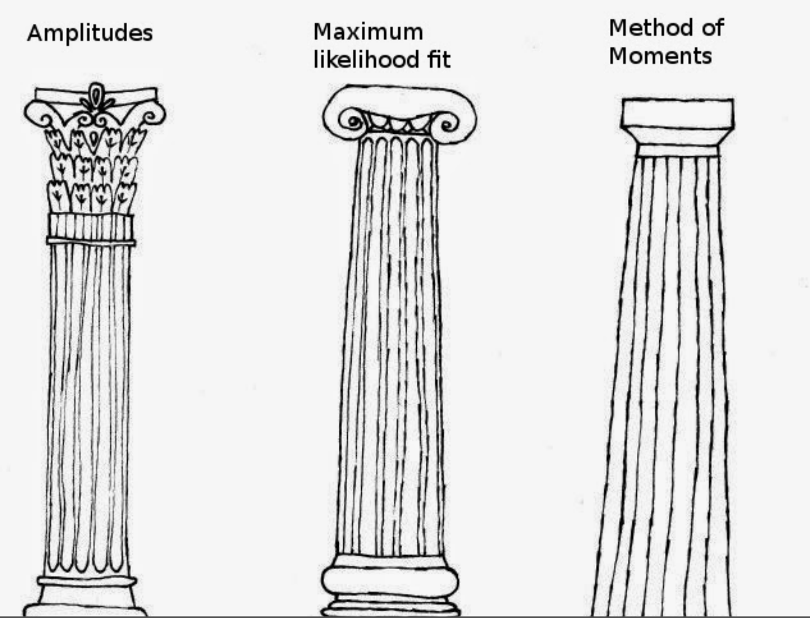

The columns of New Physics

1. Maximum likelihood fit:
   - The most standard way of obtaining the parameters.
   - Suffers from convergence problems, under coverages, etc. in low statistics.
2. Method of moments:
   - Less precise then the likelihood estimator ($10 - 15\%$ larger uncertainties).
   - Does not suffer from the problems of likelihood fit.
3. Amplitude fit:
   - Incorporates all the physical symmetries inside the amplitudes! The most precise estimator.
   - Has theoretical assumptions inside!

Maximum likelihood fit

⇛ In the maximum likelihood fit one could weight the events accordingly to the $\dfrac{1}{\varepsilon(\cos\theta_l, \cos\theta_k, \phi, q^2)}$

⇛ Better alternative is to put the efficiency into the maximum likelihood fit itself:

$$\mathcal{L} = \prod_{i=1}^{N} \epsilon_i(\Omega_i, q_i^2)\mathcal{P}(\Omega_i, q_i^2) / \int \epsilon(\Omega, q^2)\mathcal{P}(\Omega, q^2) d\Omega dq^2$$

⇛ Only the relative weights matters!

⇛ The Procedure was commissioned with TOY MC study.

⇛ Angular background component is modelled with 2^{nd} order Chebyshev polynomials, which was tested on the side-bands.

Method of moments

$\Rrightarrow$ See arXiv::1503.04100, F.Beaujean , M.Chrzaszcz, N.Serra, D. van Dyk for details.

Results in $B \to K^* \mu\mu$

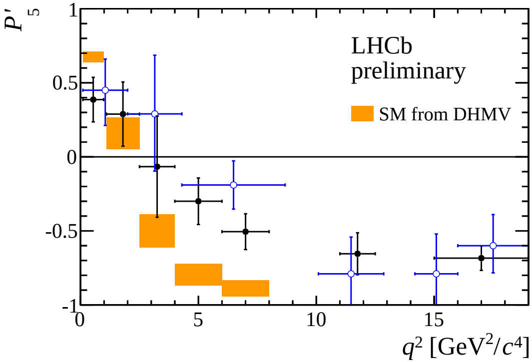

- Tension with $3\ \mathrm{fb}^{-1}$ gets confirmed!
- The two bins deviate both in $2.8\ \sigma$ from SM prediction.
- Result compatible with previous result.

Branching fraction measurements of $B \to K^{*\pm}\mu\mu$

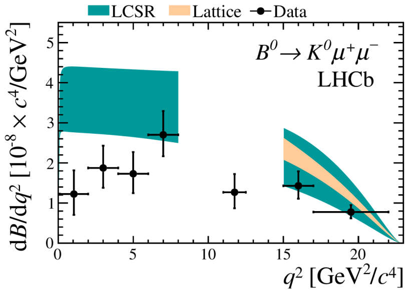

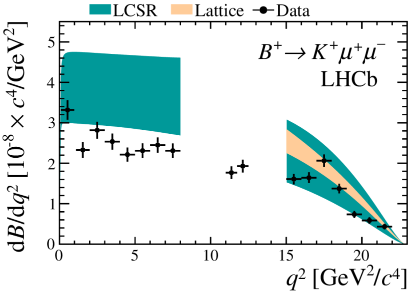

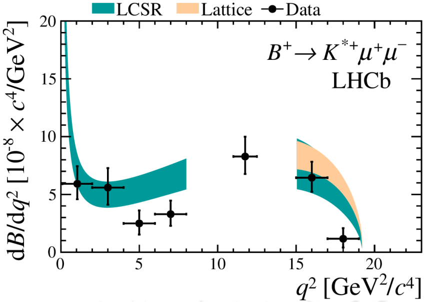

- Despite large theoretical errors the results are consistently smaller then SM prediction.

Branching fraction measurements of $B_s^0 \to \phi\mu\mu$

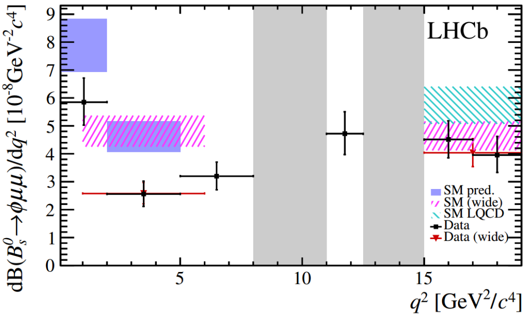

- Recent LHCb measurement [JHEPP09 (2015) 179].
- Suppressed by $\frac{f_s}{f_d}$.
- Cleaner because of narrow ϕ resonance.
- $3.3\ \sigma$ deviation in SM in the $1-6\mathrm{GeV}^2$ bin.

Branching fraction measurements of $\Lambda_b \to \Lambda\mu\mu$

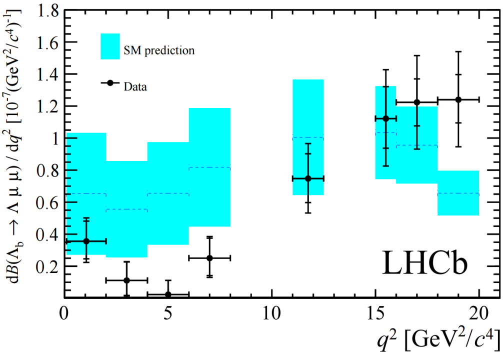

- This years LHCb measurement [JHEP 06 (2015) 115]].
- In total ~ 300 candidates in data set.
- Decay not present in the low q^2.

Branching fraction measurements of $\Lambda_b \to \Lambda\mu\mu$

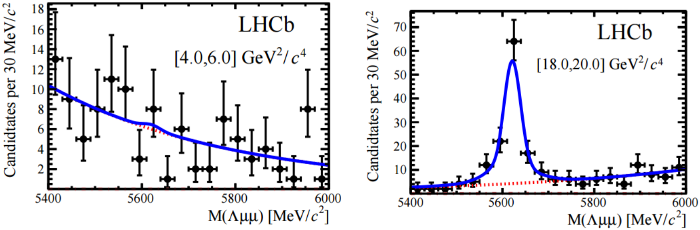

- This years LHCb measurement [JHEP 06 (2015) 115]].
- In total ~ 300 candidates in data set.
- Decay not present in the low q^2.

Angular analysis of $\Lambda_b \to \Lambda\mu\mu$

- For the bins in which we have $> 3\ \sigma$ significance the forward backward asymmetry for the hadronic and leptonic system.

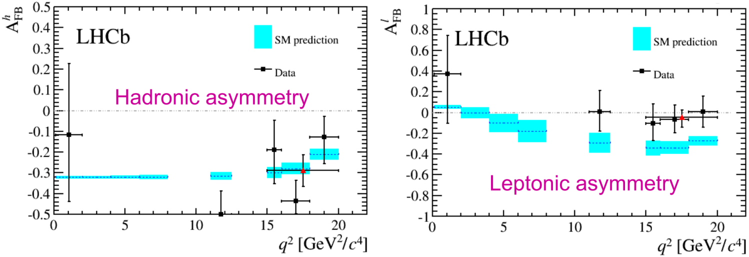

- A^H_{FB} is in good agreement with SM.
- A^ℓ_{FB} always in above SM prediction.

Lepton universality test

- If Z' is responsible for the P'_5 anomaly, does it couple equally to all flavours?

$$R_{\rm K} = \frac{\int_{q^2=1\,{\rm GeV}^2/c^4}^{q^2=6\,{\rm GeV}^2/c^4} ({\rm d}\mathcal{B}[B^+ \to K^+\mu^+\mu^-]/{\rm d}q^2){\rm d}q^2}{\int_{q^2=1\,{\rm GeV}^2/c^4}^{q^2=6\,{\rm GeV}^2/c^4} ({\rm d}\mathcal{B}[B^+ \to K^+e^+e^-]/{\rm d}q^2){\rm d}q^2} = 1 \pm \mathcal{O}(10^{-3})\ .$$

- Challenging analysis due to bremsstrahlung.
- Migration of events modeled by MC.
- Correct for bremsstrahlung.
- Take double ratio with $B^+ \to J/\psi K^+$ to cancel systematics.
- In $3{\rm fb}^{-1}$, LHCb measures $R_K = 0.745^{+0.090}_{-0.074}(stat.)^{+0.036}_{-0.036}(syst.)$
- Consistent with SM at 2.6σ.

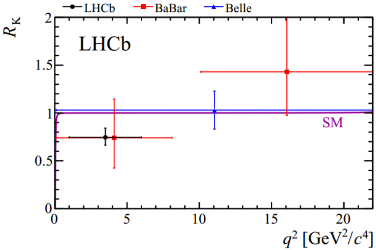

- Phys. Rev. Lett. 113, 151601 (2014)

Angular analysis of $B^0 \to K^* ee$

- With the full data set (3fb^{-1}) we performed angular analysis in $0.0004 < q^2 < 1\ \text{GeV}^2$.
- Electrons channels are extremely challenging experimentally:
  - Bremsstrahlung.
  - Trigger efficiencies.
- Determine the angular observables: $F_{\rm L}$, $A_{\rm T}^{(2)}$, $A_{\rm T}^{\rm Re}$, $A_{\rm T}^{\rm Im}$:

$$\begin{aligned} F_{\rm L} &= \frac{|A_0|^2}{|A_0|^2 + |A_{||}|^2 + |A_{\perp}|^2} \\ A_{\rm T}^{(2)} &= \frac{|A_{\perp}|^2 - |A_{||}|^2}{|A_{\perp}|^2 + |A_{||}|^2} \\ A_{\rm T}^{\rm Re} &= \frac{2\mathcal{R}e(A_{||L}A^*_{\perp L} + A_{||R}A^*_{\perp R})}{|A_{||}|^2 + |A_{\perp}|^2} \\ A_{\rm T}^{\rm Im} &= \frac{2\mathcal{I}m(A_{||L}A^*_{\perp L} + A_{||R}A^*_{\perp R})}{|A_{||}|^2 + |A_{\perp}|^2}, \end{aligned} \tag{5}$$

Angular analysis of $B^0 \to K^* ee$

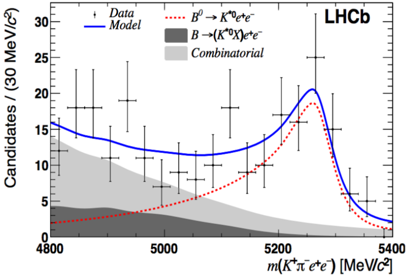

- Results in full agreement with the SM.
- Similar strength on C_7 Wilson coefficient as from $b \to s\gamma$ decays.

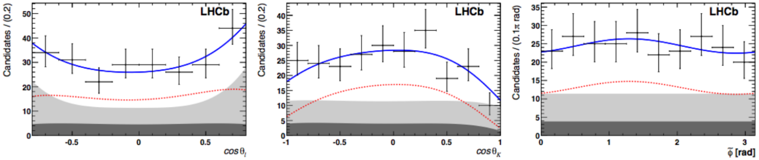

Theory implications

Theory implications

- A preliminary fit prepared by `S. Descotes-Genon, L. Hofer, J. Matias, J. Virto`, presented at 1510.04239
- Took into the fit:
  - $\mathcal{B}(B \to X_s \gamma) = (3.36 \pm 0.23) \times 10^{-4}$, Misiak et. al. 2015.
  - $\mathcal{B}(B \to \mu\mu)$, theory: Bobeth et al 2013, experiment: LHCb+CMS average (2015)
  - $\mathcal{B}(B \to X_s \mu\mu)$, Huber et al 2015
  - $\mathcal{B}(B \to K \mu\mu)$,Bouchard et al 2013, 2015
  - $PB_{(s)} \to K^*(\phi)\mu\mu$, Horgan et al 2013
  - $B \to Kee$, $B \to K^*ee$ and R_k.
- Overall there is around $4.5\ \sigma$ discrepancy wrt. SM.

Theory implications

- A preliminary fit prepared by `S. Descotes-Genon, L. Hofer, J. Matias, J. Virto`, presented at 1510.04239
- The data can be explained by modifying the C_9 Wilson coefficient.
- Overall there is around $4.5\ \sigma$ discrepancy wrt. SM.

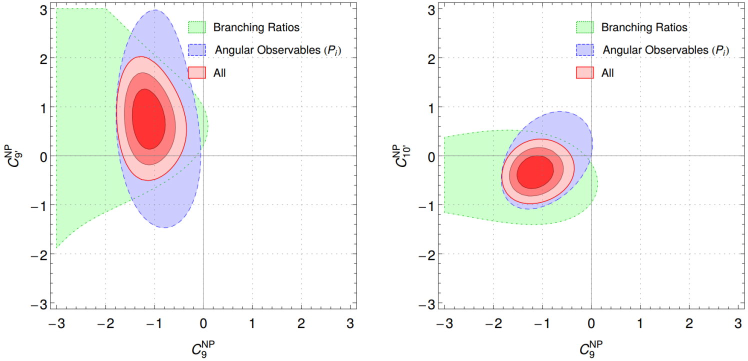

Theory implications

Coefficient	Best fit	1σ	3σ	Pull_{SM}	p-value (%)
$\mathcal{C}_7^{\text{NP}}$	-0.02	$[-0.04, -0.00]$	$[-0.07, 0.04]$	1.1	16.0
$\mathcal{C}_9^{\text{NP}}$	-1.11	$[-1.32, -0.89]$	$[-1.71, -0.40]$	**4.5**	62.0
$\mathcal{C}_{10}^{\text{NP}}$	0.58	$[0.34, 0.84]$	$[-0.11, 1.41]$	2.5	25.0
$\mathcal{C}_{7'}^{\text{NP}}$	0.02	$[-0.01, 0.04]$	$[-0.05, 0.09]$	0.7	15.0
$\mathcal{C}_{9'}^{\text{NP}}$	0.49	$[0.21, 0.77]$	$[-0.33, 1.35]$	1.8	19.0
$\mathcal{C}_{10'}^{\text{NP}}$	-0.27	$[-0.46, -0.08]$	$[-0.84, 0.28]$	1.4	17.0
$\mathcal{C}_9^{\text{NP}} = \mathcal{C}_{10}^{\text{NP}}$	-0.21	$[-0.40, 0.00]$	$[-0.74, 0.55]$	1.0	16.0
$\mathcal{C}_9^{\text{NP}} = -\mathcal{C}_{10}^{\text{NP}}$	-0.69	$[-0.88, -0.51]$	$[-1.27, -0.18]$	**4.1**	55.0
$\mathcal{C}_{9'}^{\text{NP}} = \mathcal{C}_{10'}^{\text{NP}}$	-0.09	$[-0.35, 0.17]$	$[-0.88, 0.66]$	0.3	14.0
$\mathcal{C}_{9'}^{\text{NP}} = -\mathcal{C}_{10'}^{\text{NP}}$	0.20	$[0.08, 0.32]$	$[-0.15, 0.56]$	1.7	19.0
$\mathcal{C}_9^{\text{NP}} = -\mathcal{C}_{9'}^{\text{NP}}$	-1.09	$[-1.28, -0.88]$	$[-1.62, -0.42]$	**4.8**	72.0
$\mathcal{C}_9^{\text{NP}} = -\mathcal{C}_{10}^{\text{NP}} = -\mathcal{C}_{9'}^{\text{NP}} = -\mathcal{C}_{10'}^{\text{NP}}$	-0.68	$[-0.49, -0.49]$	$[-1.36, -0.15]$	3.9	50.0
$\mathcal{C}_9^{\text{NP}} = -\mathcal{C}_{10}^{\text{NP}} = \mathcal{C}_{9'}^{\text{NP}} = -\mathcal{C}_{10'}^{\text{NP}}$	-0.17	$[-0.29, -0.06]$	$[-0.54, 0.18]$	1.5	18.0

Table 2: *Best-fit points, confidence intervals, pulls for the SM hypothesis and p-values for different one-dimensional NP scenarios.*

If not NP?

- We are not there yet!
- There might be something not taken into account in the theory.
- Resonances (J/ψ, $\psi(2S)$) tails can mimic NP effects.
- There might be some non factorizable QCD corrections.
  " However, the central value of this effect would have to be significantly larger than expected on the basis of existing estimates" `D.Straub, 1503.06199` .

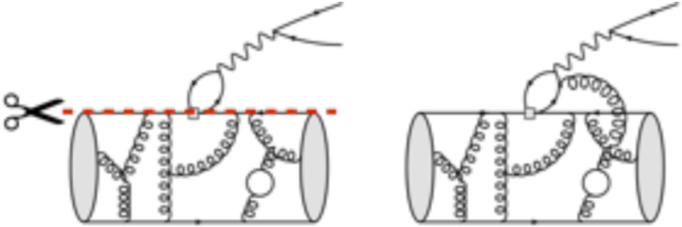

If not NP?

- We are not there yet!
- There might be something not taken into account in the theory.
- Resonances (J/ψ, $\psi(2S)$) tails can mimic NP effects.
- There might be some non factorizable QCD corrections.
  " However, the central value of this effect would have to be significantly larger than expected on the basis of existing estimates" `D.Straub, 1503.06199` .

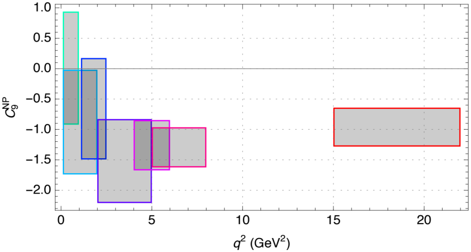

If not NP?

- How about our clean P_i observables?
- The QCD cancel as mentioned only at leading order.
- Comparison to normal observables with the optimised ones.

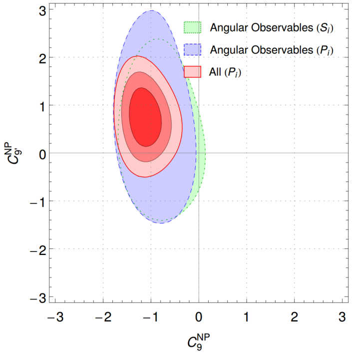

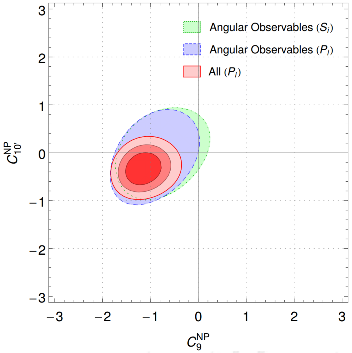

There is more!

- There is one other LUV decay recently measured by LHCb.
- $R(D^*) = \dfrac{\mathcal{B}(B \to D^*\tau\nu)}{\mathcal{B}(B \to D^*\mu\nu)}$
- Clean SM prediction: $R(D^*) = 0.252(3)$, PRD 85 094025 (2012)
- LHCb result: $R(D^*) = 0.336 \pm 0.027 \pm 0.030$, HFAG average: $R(D^*) = 0.322 \pm 0.022$
- $3.9\ \sigma$ discrepancy wrt. SM.

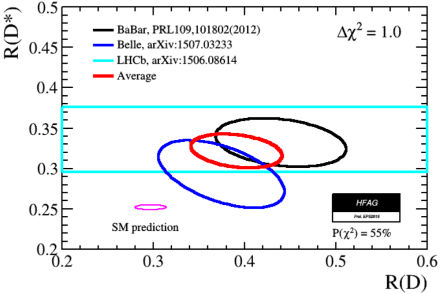

Conclusions

- Clear tensions wrt. SM predictions!
- Measurements cluster in the same direction.
- We are not opening the champagne yet!
- Still need improvement both on theory and experimental side.
- Time will tell if this is QCD+fluctuations or new Physics:

Conclusions

- Clear tensions wrt. SM predictions!
- Measurements cluster in the same direction.
- We are not opening the champagne yet!
- Still need improvement both on theory and experimental side.
- Time will tell if this is QCD+fluctuations or new Physics:

"... when you have eliminated all the
Standard Model explanations, whatever remains,
however improbable, must be New Physics."
prof. Joaquim Matias

Thank you for the attention!

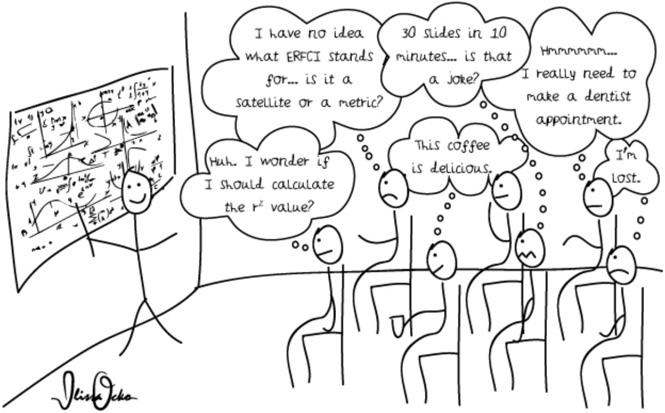

Backup

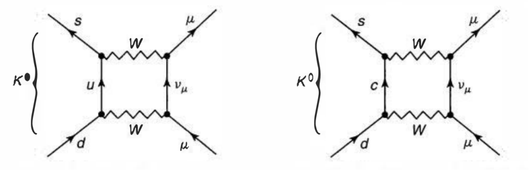

- Cabibbo angle was successful in explaining dozens of decay rates in the 1960s.
- There was, however, one that was not observed by experiments: $K^0 \to \mu^- \mu^+$.
- Glashow, Iliopoulos, Maiani (GIM) mechanism was proposed in the 1970 to fix this problem. The mechanism required the existence of the 4^{th} quark.
- At that point most of the people were skeptical about that. Fortunately in 1974 the discovery of the J/ψ meson silenced the skeptics.

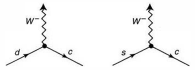

$$\frac{-ig_w}{2\sqrt{2}}\gamma^\mu(1-\gamma^5)(-\sin\theta_C) \qquad \frac{-ig_w}{2\sqrt{2}}\gamma^\mu(1-\gamma^5)\cos\theta_C$$

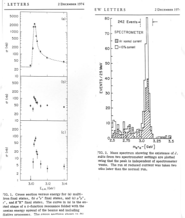

A lesson from history - CKM matrix

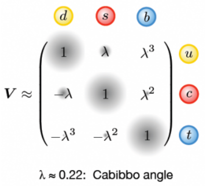

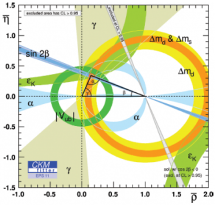

- Similarly CP violation was discovered in 1960s in the neutral kaons decays.
- 2×2 Cabbibo matrix could not allow for any CP violation.
- For the CP violation to be possible one needs at least a 3×3 unitary matrix $\looparrowright$ Cabibbo-Kobayashi-Maskawa matrix (1973).
- It predicts existence of b (1977) and t (1995) quarks.

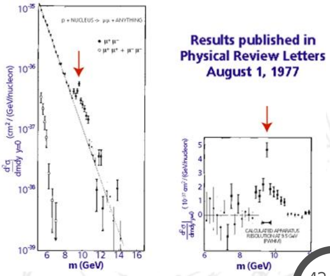

A lesson from history - Weak neutral current

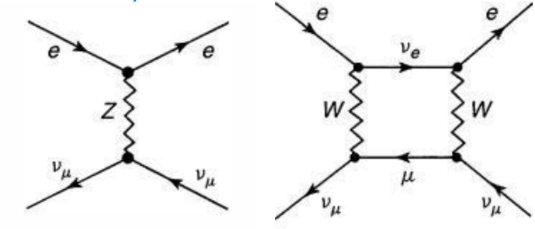

- Weak neutral currents were first, introduced in 1958 by Buldman.
- Later on they were naturally incorporated into unification of weak and electromagnetic interactions.
- ’t Hooft proved that the GWS models was renormalizable.
- Everything was there on theory side, only missing piece was the experiment, till 1973.

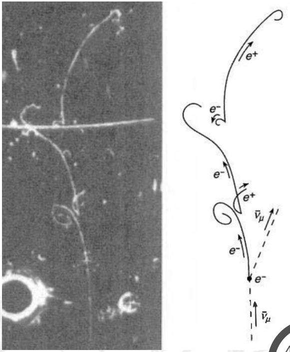

Recent measurements

⇛ Branching fractions:

$B^{0,\pm} \to K^{0,\pm}\mu^-\mu^+$ LHCb, Mar 14

$B^0 \to K^*\mu^-\mu^+$ CMS, Jul 15

$B_s^0 \to \phi\mu^-\mu^+$ LHCb, Jun 15

$B^\pm \to \pi^\pm\mu^-\mu^+$ LHCb, Sep 15

$\Lambda_b \to \Lambda\mu^-\mu^+$ LHCb, Mar 15

$B \to \mu^-\mu^+$ CMS+LHCb, Jun 15

⇛ CP asymmetry:

$B^\pm \to \pi^\pm\mu^-\mu^+$ LHCb, Sep 15

⇛ Isospin asymmetry:

$B \to K\mu^-\mu^+$ LHCb, Mar 14

⇛ Lepton Universality:

$B^\pm \to K^\pm\ell\bar{\ell}$ LHCb, Jun 14

⇛ Angular:

$B^0 \to K^*\ell\bar{\ell}$ LHCb, Jan 15

$B^\pm \to K^{*,\pm}\ell\bar{\ell}$ BaBar, Aug 15

$B_s^0 \to \phi\ell\bar{\ell}$ LHCb, Jun 15

$\Lambda_b \to \Lambda\mu^-\mu^+$ LHCb, Mar 15

Recent measurements

⇛ Branching fractions:

$B^{0,\pm} \to K^{0,\pm}\mu^-\mu^+$ LHCb, Mar 14

$B^0 \to K^*\mu^-\mu^+$ CMS, Jul 15

$B_s^0 \to \phi\mu^-\mu^+$ LHCb, Jun 15

$B^\pm \to \pi^\pm\mu^-\mu^+$ LHCb, Sep 15

$\Lambda_b \to \Lambda\mu^-\mu^+$ LHCb, Mar 15

$B \to \mu^-\mu^+$ CMS+LHCb, Jun 15

⇛ CP asymmetry:

$B^\pm \to \pi^\pm\mu^-\mu^+$ LHCb, Sep 15

⇛ Isospin asymmetry:

$B \to K\mu^-\mu^+$ LHCb, Mar 14

⇛ Lepton Universality:

$B^\pm \to K^\pm\ell\bar{\ell}$ LHCb, Jun 14

⇛ Angular:

$B^0 \to K^*\ell\bar{\ell}$ LHCb, Jan 15

$B^\pm \to K^{*,\pm}\ell\bar{\ell}$ BaBar, Aug 15

$B_s^0 \to \phi\ell\bar{\ell}$ LHCb, Jun 15

$\Lambda_b \to \Lambda\mu^-\mu^+$ LHCb, Mar 15

$> 2\ \sigma$ deviations from SM